

Zero Oxidation State Compounds of Scandium, Yttrium, and the Lanthanides

F. Geoffrey N. Cloke

School of Chemistry and Molecular Sciences, University of Sussex, Brighton BN1 9QJ, U.K.

This review will focus on organometallic and coordination compounds of scandium, yttrium, and the lanthanide elements in the zero oxidation state, isolable and crystallographically characterized examples of which have only been discovered recently. However, I will start with some introductory material summarizing the basic principles governing the chemistry of these elements, and of their compounds, in 'conventional' oxidation states.

1 Introduction to Traditional Lanthanide Chemistry

The lanthanides constitute the row of fourteen elements following lanthanum in the periodic table which have in common a xenon core electronic configuration and occupied $6s$ orbitals. The series corresponds to a gradual filling of the seven $4f$ orbitals, and the elements (and their cations) undergo a smooth decrease in radius with increasing atomic number known as the 'lanthanide contraction', a direct result of the poor ability of electrons in the f subshell to shield outer electrons from increasing nuclear charge.

A fortuitous combination of conditions conspires to make the +3 oxidation state the most stable throughout the entire series, and indeed the study of organolanthanide chemistry in the trivalent state has been an area of considerable activity over the past fifteen years which has been extensively reviewed.¹ The stability of the f^6 , f^7 , and f^{14} electronic configurations also renders the +2 oxidation state accessible for samarium, europium, and ytterbium respectively, and divalent compounds of these elements have found considerable application in organic synthesis² and also display remarkable reactivity as one-electron reducing agents in stoichiometric organometallic reactions.³ The +4 oxidation state is found for cerium, as a consequence of the stable f^0 configuration, and Ce^{IV} compounds are employed

as powerful one-electron oxidizing agents, although this high oxidizing power of Ce^{IV} has resulted in a paucity of well-characterized organometallic compounds of cerium in this oxidation state.⁴

Although it is the $4f$ orbitals which are being filled in the lanthanide series, it is generally supposed that they do not play a significant part in the chemistry of lanthanide complexes (unlike the d orbitals of transition metals). This is because they have a limited radial extension and are shielded from the valence shell by the filled $5s$ and $5p$ orbitals. Only in the sense that loss of one $4f$ electron is usually necessary to achieve the ubiquitous +3 oxidation state of the series are they considered to play a part in reactions. Thus for most chemical reactions all the lanthanide elements present an inert gas core electronic configuration with a +3 charge. It is also for this reason that yttrium and scandium complexes are included in discussions of lanthanide chemistry, *i.e.* in their predominant +3 oxidation states these elements have an inert gas core configuration ($[Kr]$ and $[Ar]$ respectively) and empty d orbitals. Indeed, due to the lanthanide contraction, the size of Y^{3+} falls between that of Ho^{3+} and Er^{3+} , whereas scandium is considerably smaller than the lanthanides. However, compared to transition metals, the lanthanides are quite large and typically display coordination numbers of 8–12; the lanthanides are also rather more electropositive than the transition elements, and are highly oxophilic.

The combination of properties mentioned in the preceding paragraphs has important consequences for the organometallic and coordination chemistry of these elements:

Such complexes have been traditionally viewed as largely ionic, in view of the inability of the f orbitals to overlap effectively with ligand molecular orbitals.

Unlike the transition metals, all the members of the series display similar chemical behaviour, differing only in degree due to changes in size. Thus the potential exists to tune the reaction site for a given reaction simply by changing the lanthanide and hence the radius of the central metal.

Also in contrast to transition metal chemistry, oxidative-addition reactions are expected to be unfavourable, since a selection of oxidation states is not readily available.

The small role of covalent interactions in conventional lanthanide chemistry presents possibilities for new types of reactivity not observed for d -block metals, without the restrictions imposed by the need for compatible orbital symmetries.

The large radii of the lanthanide elements mean that sterically demanding ligands are usually required to obtain discrete, monomeric compounds.

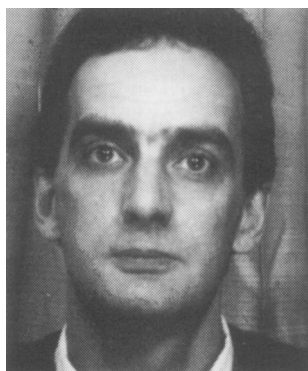
From a practical standpoint, lanthanide complexes are virtually all extremely oxygen and moisture sensitive, requiring rigorous manipulation techniques.

2 Background to Lanthanide (0) Compounds

2.1 Bonding Aspects

The stabilization of zero oxidation state transition metal compounds is classically achieved by the use of π -acceptor ligands such as carbon monoxide or arenes, capable of accepting electron density from the metal centre *via* back-donation from suitable, filled metal d -orbitals. The latter prevents unacceptable build-up of charge on the metal centre and consequent violation of the electroneutrality principle. In view of the fact that the $4f$

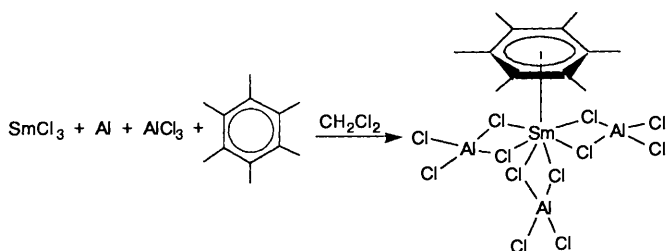
Geoff Cloke received his D.Phil. in 1978 from Oxford University, where he studied under the supervision of Professor M. L. H. Green. He then stayed in Oxford as a Junior Research Fellow at Balliol College during the tenure of a Ramsay Memorial Fellowship. During this time he also spent one year at the Massachusetts Institute of Technology working with Professor R. R. Schrock. In 1984 he took up a New Blood Lectureship at the University of Sussex, and was promoted to a Senior Lectureship in 1989 and subsequently to a Readership in 1990. He is a past recipient of the Sir Edward Frankland Fellowship (1988–1989) and was awarded the Corday-Morgan Medal in 1990. His research interests lie in the field of early transition metal and f-element organometallic chemistry, and in particular the use of metal vapour synthesis to prepare novel compounds of these elements in unusual oxidation states and ligand environments.



orbitals have poor radial extension and are essentially core orbitals (*vide supra*), the potential for using them for such back-donation to stabilize a lanthanide(0) compound seemed very limited. However, consideration of lanthanide atomic spectra shows that the $4f$ and $5d$ levels are quite similar in energy, and indeed the ground state of the gadolinium atom is $[\text{Xe}]4f^7 5d^1 6s^2$. Thus, assuming that the ligand-metal bond strengths are sufficient to overcome the necessary promotion energy, there exists the possibility of using electrons promoted from the $4f$ to the $5d$ level for back-bonding.

2.2 Synthetic Approaches to Lanthanide(0) Compounds

A widely employed conventional strategy for the synthesis of zero oxidation state transition metal complexes is the reduction of a suitable higher oxidation state precursor (*e.g.* a halide) in the presence of a π -acceptor ligand, for example the classic Fischer-Hafner route to bis(η -arene)metal complexes.⁵ However, the electropositive lanthanide elements have reduction potentials from the (III) to the (0) oxidation state well in excess of -2 volts, so that chemical, or indeed electrochemical, reduction as a route to lanthanide(0) species would be expected to be extremely difficult to achieve. This point is nicely illustrated by work reported by Cotton⁶ attempts to prepare bis(η -hexamethylbenzene)samarium(0) by Fischer-Hafner reduction of SmCl_3 by Al/AlCl_3 in the presence of hexamethylbenzene resulted instead in the formation of the samarium(III) complex $[\text{Sm}(\eta\text{-C}_6\text{Me}_6)(\mu^2\text{-AlCl}_4)_3]$, the first crystallographically characterized η -arene lanthanide derivative (see Scheme 1).



Scheme 1

In principle, the use of the metals themselves as starting materials offers the most attractive strategy for the synthesis of zero oxidation state lanthanide complexes. The bulk metals, either in the form of filings, ingots, or powders (sometimes activated by Hg or HgCl_2 to form amalgams) have been employed in synthesis, but this has invariably resulted in the formation of lanthanide(II)⁷ (in the case of Yb) or lanthanide(III) species.⁸ The alternative approach, and the one which has proved successful, has been to use lanthanide metal atoms as reagents, either to generate thermally unstable lanthanide(0) species in matrix isolation experiments, or to prepare isolable compounds by macroscale metal vapour synthesis. The remainder of this review will therefore concentrate on these two approaches, and in particular the latter.

3 Matrix Isolation Studies of Lanthanide Atoms

3.1 Reactions with Carbon Monoxide

Early work in this area by Slater and Shelton demonstrated the existence of a variety of lanthanide carbonyl complexes of the type $\text{Ln}(\text{CO})_n$ ($\text{Ln} = \text{Pr}, \text{Nd}, \text{Eu}, \text{Gd}, \text{Yb}, n = 1-6$)⁹ However, the extreme thermal instability of these species ($\text{dec} > 20 \text{ K}$) precluded unambiguous characterization, other than by detailed infra-red spectroscopy.

3.2 Reactions with Ethene

More recently, Wayda¹⁰ has demonstrated the existence of europium-ethene species, synthesized at 12 K by the co-deposi-

tion of Eu atoms with ethene, neat or diluted with Ar or Xe . These complexes, of the type $\text{Eu}(\text{C}_2\text{H}_4)$ and $\text{Eu}(\text{C}_2\text{H}_4)_n$, decomposed above 50 K , and were characterized by UV/VIS and IR spectroscopy. Molecular orbital calculations indicated that the ethene ligand in $\text{Eu}(\text{C}_2\text{H}_4)$ is only weakly bonded by back donation from a europium f orbital into the olefin π^* system, with little forward donation from the olefin σ or π orbitals.

3.3 Reactions with Arenes

A recent investigation¹¹ into the reactivity of scandium atoms in hydrocarbon matrices examined the co-condensation reactions of scandium with both inert (adamantane, cyclohexane, and deuterocyclohexane) and reactive (benzene, deuterobenzene, and cyclohexene) co-reactants, using a rotating cryostat at 77 K . ESR measurements indicated that the paramagnetic products formed in the 'inert' matrices were weakly bonded $\text{Sc}-\text{H}$ species. The co-deposition of scandium atoms with benzene led to two ESR active species: one possessed a large scandium hyperfine coupling and is believed to be a complex of the type $\text{Sc}(\eta\text{-C}_6\text{H}_6)_n$, $n = 1$ or 2 , and the second product is thought to arise from the interaction of a scandium atom with only one double bond of the benzene molecule, since a similar spectrum was obtained with cyclohexene.

4 Macroscale Synthetic Reactions of Lanthanide Atoms

The technique of metal vapour synthesis, in which metal vapour generated under high vacuum conditions is co-condensed with a potential ligand at 77 K , has found considerable application in the synthesis of novel compounds unobtainable by classical methods. It is particularly applicable to the synthesis of zero oxidation state complexes, *e.g.* bis(η -arene) compounds of the electropositive early transition metals.^{12,13} The technique has been well reviewed¹⁴ and will not be discussed in detail here. However, vaporization of some of the lanthanides does present a particular difficulty, associated with the electropositive nature of these elements: whilst most of the lanthanides have vaporization temperatures under high vacuum well below the temperature limit (1800°C) for resistively heated oxide crucibles, only those lanthanides which sublime under vacuum ($\text{Sm}, \text{Eu}, \text{Dy}, \text{Ho}, \text{Tm}$, and Yb) may be cleanly evaporated by this method. The remaining elements ($\text{Sc}, \text{Y}, \text{La}, \text{Ce}, \text{Pr}, \text{Nd}, \text{Gd}, \text{Tb}, \text{Er}$, and Lu) melt before attaining a suitable vaporization temperature and, when molten, will chemically reduce oxide crucibles or alloy with metal boats. Investigation of the atom chemistry of these metals on a reasonable scale therefore requires the use of a 'containerless' method for evaporation, namely the positive hearth electron beam furnace.¹²

4.1 Reactions with Alkenes and Alkynes

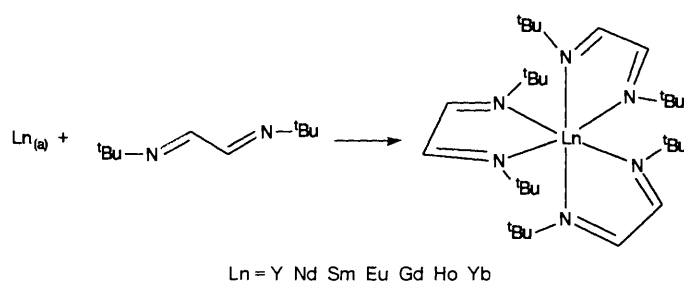
Initial work on lanthanide metal vapour reactivity by Evans,³ directed towards the synthesis of stable lanthanide(0) species, examined the reactions of lanthanide atoms with a variety of unsaturated hydrocarbons. Reactions of Nd or Er with 3-hexyne gave products of composition $\text{Ln}_2(3\text{-hexyne})_3$, whereas with Sm or Yb the products were of stoichiometry $\text{Ln}(3\text{-hexyne})$. Similarly, with butadiene, Nd, Sm , or Er afforded materials analysing as $\text{Ln}(\text{butadiene})_3$, but 2,3-dimethyl substitution of the butadiene ligand yielded products whose composition was $\text{Ln}(2,3\text{-dimethylbutadiene})_2$, $\text{Ln} = \text{La}, \text{Nd}, \text{Sm}$, or Er . These products were all intensely coloured and exhibited magnetic moments outside the range usually associated with the respective lanthanide(III) ion values. However, the complex behaviour of these materials in solution indicated that they were oligomeric in nature, and none of the species could be structurally characterized. Hence their precise nature remains unclear, although the products from the lanthanide atom co-condensation reactions with 3-hexyne or 2,3-dimethylbutadiene were found to be catalytically active for the *cis* hydrogenation of alkynes.

In the case of the reactions of lanthanide atoms with ethene, propene, or 1,2-propadiene, only erbium was found to yield soluble products. Hydrolytic studies of the complex reaction mixtures indicated that alkene polymerization and insertion were occurring in these reactions together with C–H bond activation.³

4.2 Synthesis and structures of 1,4-Diazabutadiene Complexes

This class of ligand, of the general $\text{RN}=\text{CH}-\text{CH}=\text{NR}$, has found extensive and varied application in transition metal coordination chemistry.¹⁵ One of the principal modes of bonding of these ligands is σ -coordination to a metal *via* the lone pairs on the two nitrogen atoms to form a five membered highly stabilized, planar ring system, in which the existence of a low-lying ligand π^* orbital stabilizes low oxidation state compounds *via* π -acceptor bonding.

The reaction of a variety of lanthanide metal vapours with 1,4-di-*t*-butyldiazabutadiene has been found to yield the deep green trischelate, formally lanthanide(0) compounds $[\text{Ln}(\text{Bu}^t\text{DAB})_3]$ ($\text{Ln} = \text{Y}, \text{Nd}, \text{Sm}, \text{Eu}, \text{Gd}, \text{Ho}, \text{Yb}$, $\text{Bu}^t\text{DAB} = 1,4\text{-di-}t\text{-butyldiazabutadiene}$), see Scheme 2.¹⁶ With the less sterically demanding 1,4-di-*i*-propyldiazabutadiene, the analogous products were found to be thermally unstable above 0 °C.¹⁷



Scheme 2

The structure of the samarium derivative has been determined by *X*-ray crystallography, and is shown in Figure 1.¹⁸

The overall geometry about the samarium centre is octahedral, and the $\text{Sm}-\text{N}=\text{C}-\text{C}=\text{N}$ chelate ring is almost planar with a maximum out-of-plane deviation of 0.051 Å. The average $\text{Sm}-\text{N}$ distance, 2.419(16) Å, is considerably shorter than that expected for a $\text{Sm}^{\text{III}}-\text{N}$ or $\text{Sm}^{\text{II}}-\text{N}$ single bond, and is closer to the value expected for a $\text{Sm}^{\text{III}}-\text{N}$ single bond. The main feature of interest is the average $\text{C}=\text{N}$ bond distance of 1.35(3) Å in the DAB skeleton, a significant increase to that in the free ligand [1.283(6) Å]. This increase is associated with substantial

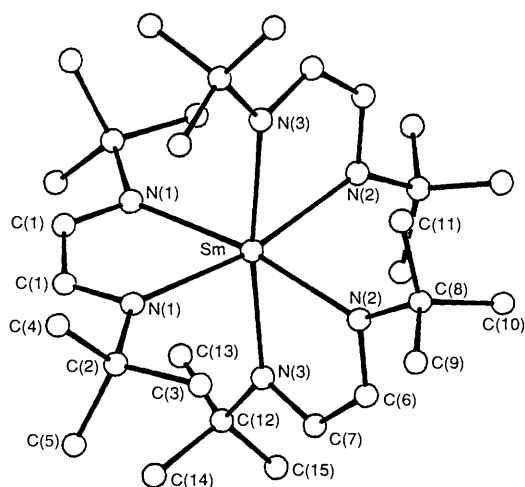


Figure 1 Molecular structure of $[\text{Sm}(\text{Bu}^t\text{DAB})_3]$

delocalization of metal electron density into the antibonding LUMO of the ligand. Hence $[\text{Sm}(\text{Bu}^t\text{DAB})_3]$ and the other lanthanide analogues, although *formally* M^0 complexes, are best formulated as M^{III} complexes, *viz.* $[\text{Ln}^{3+}(\text{Bu}^t\text{DAB})_3]$, a reflection of the ease of reduction of the ligand to its radical anion by the electropositive lanthanides. This is also in accord with the ESR spectrum of the yttrium analogue: no coupling to yttrium (^{89}Y , $I = 1/2$, 100%) was observed, and the spectrum at 420 K only exhibited coupling of one unpaired electron to six equivalent nitrogen nuclei with a g -value very close to the free spin value, again indicative of $[\text{Y}^{3+}(\text{Bu}^t\text{DAB})_3]$. $[\text{Yb}(\text{Bu}^t\text{DAB})_3]$ has also been the subject of a solid state magnetic study: the room temperature magnetic moment was found to be 5.9 BM, whereas below 100 K the compound exhibited a magnetic moment of 2.4 BM. This spin equilibrium has been rationalized in terms of $[\text{Yb}(\text{Bu}^t\text{DAB})_3]$ existing as the Yb^{III} species $[\text{Yb}^{3+}(\text{Bu}^t\text{DAB})_3]$ above 100 K, and as the Yb^{II} species $[\text{Yb}^{2+}(\text{Bu}^t\text{DAB})_2(\text{Bu}^t\text{DAB})]$ below this temperature, for which the calculated magnetic moments of 5.5 and 2.45 BM, respectively, are in good agreement with the experimental values.¹⁹

The reaction of scandium vapour with Bu^tDAB resulted in the formation of the bis(ligand) complex $[\text{Sc}(\text{Bu}^t\text{DAB})_2]$,²⁰ a reflection of the smaller size of scandium compared with yttrium and the lanthanides. Although this product was not structurally authenticated, the structure shown in Figure 2, in which one of the Bu^tDAB ligands has been doubly reduced to the $\text{Bu}^t-\text{N}=\text{CH}-\text{CH}=\text{N}-\text{Bu}^t$ dianion, has been proposed on the basis of magnetic and ESR data, and by analogy with that of the Al and Ga derivatives.²¹

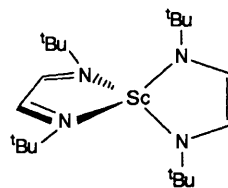


Figure 2 Proposed structure of $[\text{Sc}(\text{Bu}^t\text{DAB})_2]$

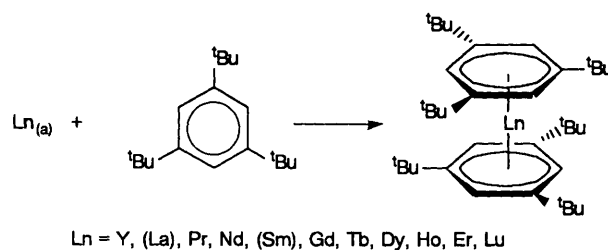
$[\text{Sc}(\text{Bu}^t\text{DAB})_2]$ is thus formally a compound of Sc^{II} , although once again the unpaired electron density resides in the ligand π^* orbital and the compound is thus realistically classed as Sc^{III} .

4.3 1,3,5-Tri-*t*-butylbenzene Complexes

4.3.1 Synthesis and Structure

The co-condensation of yttrium or gadolinium vapour with 1,3,5-tri-*t*-butylbenzene (Bz^*) afforded the stable, crystalline zero oxidation state sandwich compounds $[\text{M}(\eta\text{-Bz}^*)_2]$, $\text{M} = \text{Y}$ or Gd , the gadolinium compound representing the first unambiguous *f*-element(0) complex.²²

Subsequently the reactions of the remaining lanthanide vapours with Bz^* were examined, which yielded stable analogues for several of the elements (see Scheme 3 and Table 1).²³ Physical data for $[\text{Sc}(\eta\text{-Bz}^*)_2]$ are also included in Table 1, but the unusual products of the reaction between scandium atoms and Bz^* will be discussed at the end of this Section. The stability



Scheme 3

Table 1 Stability and some physical properties of $[\text{Ln}(\eta\text{-Bz}^*)_2]$ complexes

Atom	Ground State	Colour	$\lambda_{\text{max}}(\text{nm})^a$	Stability ^b
Sc	d^1s^2	orange	495	stable
Y	d^1s^2	purple	529	stable
La	d^1s^2	green	637	dec $> 0^\circ\text{C}$
Ce	$f^1d^1s^2$	—	—	unstable
Pr	f^3s^2	purple	541	dec $> 40^\circ\text{C}$
Nd	f^4s^2	blue	544	stable
Sm	f^6s^2	green	691	dec $> -30^\circ\text{C}$
Eu	f^7s^2	—	—	unstable
Gd	$f^7s^2d^1s^2$	purple	542	stable
Tb	f^9s^2	purple	540	stable
Dy	$f^{10}s^2$	purple	556	stable
Ho	$f^{11}s^2$	deep pink	507	stable
Er	$f^{12}s^2$	red	499	stable
Tm	$f^{13}s^2$	—	—	unstable
Yb	$f^{14}s^2$	—	—	unstable
Lu	$f^{14}d^1s^2$	red-brown	495	stable

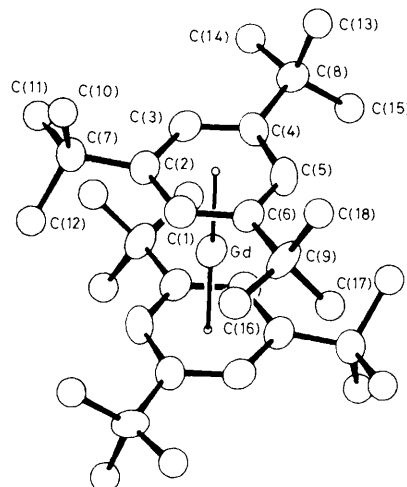
Measured in pentane solution ^a Stable \Rightarrow dec $> 100^\circ\text{C}$
 unstable \Rightarrow insoluble from the metal atom reactor at any convenient temperature

trend of the $[\text{Ln}(\eta\text{-Bz}^*)_2]$ compounds across the lanthanide series will be discussed in Section 4.3.2

The $[\text{Ln}(\eta\text{-Bz}^*)_2]$ complexes are all extremely air sensitive crystalline solids, very soluble in hydrocarbon solvents, and are highly coloured, a feature associated with their characteristic intense band ($\epsilon > 10^4$) in the visible region of the spectrum. The latter has been assigned to a ligand-to-metal charge-transfer (LMCT) transition, which will be discussed in Section 4.4. The f^0 yttrium complex is ESR-silent at room temperature by virtue of its proposed rapidly relaxing 2E ground state (discussed in detail in Section 4.3.2), but displayed a frozen solution spectrum at 77 K exhibiting a doublet coupling to yttrium, confirming unpaired electron density on the yttrium centre in this genuine Y^0 compound (*cf* $[\text{Y}(\text{Bu}^1\text{DAB})_3]$ in Section 4.2). In the case of the f^{14} lutetium analogue, a weak octet (^{175}Lu , 97%, $I = 7/2$) was observable at room temperature in the ESR spectrum, presumably the result of a somewhat longer relaxation time.

The molecular structure of $[\text{Gd}(\eta\text{-Bz}^*)_2]$ has been determined by X-ray crystallography, and is shown in Figure 3.

The structure shows that $[\text{Gd}(\eta\text{-Bz}^*)_2]$ has the classic parallel ring sandwich structure, typical of its d -block analogues. The gadolinium atom lies on a centre of symmetry, with the planar arene rings eclipsed in order to minimize *t*-butyl group interactions. The *t*-butyl groups are bent out of the plane of the arene rings by $6\text{--}10^\circ$, as has been observed with ring-substituted bis(η -arene) transition metal complexes, and attributable to the ring carbons becoming more sp^3 in character on binding to the metal. Two of the three methyl groups of each *t*-butyl substituent are located between the planes defined by the arene rings, thus surrounding the metal centre by twelve methyl groups, and presumably accounting for the kinetic stability of the compound. The Gd–ring–C distances range from 2.585(4) to 2.660(4) Å [average 2.630(4) Å], significantly shorter than the average corresponding distance of 2.89(5) Å found in $[\text{Sm}(\eta\text{-$

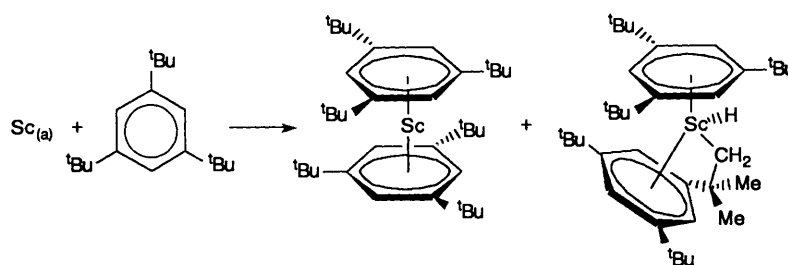
**Figure 3** The X-ray structure of $[\text{Gd}(\eta\text{-Bu}^1_3\text{C}_6\text{H}_3)_2]$

$\text{C}_6\text{Me}_6)(\mu^2\text{-AlCl}_4)_6$, despite the fact that Sm^{III} is considerably smaller than Gd^0 . Indeed, the arene–metal bond in $[\text{Sm}(\eta\text{-C}_6\text{Me}_6)(\mu^2\text{-AlCl}_4)]$ (see Section 2.2) has been described in terms of a weak electrostatic interaction between the π -system of hexamethylbenzene and the Sm^{III} centre, whereas the bond in $[\text{Gd}(\eta\text{-Bz}^*)_2]$ is clearly much more akin to that of $[\text{Cr}(\eta\text{-C}_6\text{H}_6)_2]$ in which the M–ring–C distance is 2.142(2) Å,²⁴ given the relative sizes of Gd and Cr. The bond angles in the arene rings are not perturbed (within standard deviations) from those of the free ligand, but the average ring C–C distances are slightly longer, again, the latter effect is also observed in $[\text{Cr}(\eta\text{-C}_6\text{H}_6)_2]$. The bonding in the $[\text{Ln}(\eta\text{-Bz}^*)_2]$ compounds will be discussed in the next Section.

The holmium analogue was found to be isostructural with $[\text{Gd}(\eta\text{-Bz}^*)_2]$. The one salient difference lies in the average M–ring–C distance, that for the holmium compound [2.580(3) Å] being 0.05 Å shorter, an effect attributed to the smaller radius of holmium, arising from the lanthanide contraction.

The reaction between scandium atoms and 1,3,5-tri-*t*-butylbenzene gave an unexpected result in yielding not only the Sc^0 sandwich compound $[\text{Sc}(\eta\text{-Bz}^*)_2]$, but also a similarly unique example of Sc^{II} , $[\text{Sc}(\eta\text{-Bz}^*)(\eta^6, \eta^1\text{-Bu}^1_2\{\text{CMe}_2\text{CH}_2\}\text{C}_6\text{H}_3)\text{H}]$, see Scheme 4.²⁵

$[\text{Sc}(\eta\text{-Bz}^*)_2]$ exhibits ESR behaviour analogous to that of the yttrium analogue: the compound was found to be ESR-silent at room temperature, but displayed a frozen solution spectrum showing hyperfine coupling to ^{45}Sc (100%, $I = 7/2$). Whilst pure $[\text{Sc}(\eta\text{-Bz}^*)_2]$ could be obtained by sublimation of the product mixture, $[\text{Sc}(\eta\text{-Bz}^*)(\eta^6, \eta^1\text{-Bu}^1_2\{\text{CMe}_2\text{CH}_2\}\text{C}_6\text{H}_3)\text{H}]$ decomposed under these conditions, and other separation procedures were found to be ineffectual (fractional crystallization) or resulted in decomposition (chromatography). Thus the assignment of the second, purple, product as the 17-electron Sc^{II} complex $[\text{Sc}(\eta\text{-Bz}^*)(\eta^6, \eta^1\text{-Bu}^1_2\{\text{CMe}_2\text{CH}_2\}\text{C}_6\text{H}_3)\text{H}]$ was made on the basis of its solution ESR spectrum (octet of doublets of triplets, arising from hyperfine coupling to ^{45}Sc , $-\text{H}$, and $-\text{CH}_2$, respectively) supported by a simulation, and its visible

**Scheme 4**

absorption spectrum ($\lambda_{\max} = 557 \text{ nm}$, $\epsilon = 10^4$). Surprisingly it was not found possible to interconvert $[\text{Sc}(\eta\text{-Bz}^*)_2]$ and $[\text{Sc}(\eta\text{-Bz}^*)(\eta^6, \eta^1\text{-Bu}^2_2\{\text{CMe}_2\text{CH}_2\}\text{C}_6\text{H}_3)\text{H}]$ either thermally or photochemically, although the latter compound formally arises from insertion of the scandium centre into a methyl group of one of the *t*-butyl ring substituents in $[\text{Sc}(\eta\text{-Bz}^*)_2]$. However, whilst the ratio of the two products was found to be 8:1 in favour of the normal sandwich compound when the co-condensation reaction was carried out at 77 K, co-condensation at 195 K resulted in an equimolar mixture of the two. The formation of $[\text{Sc}(\eta\text{-Bz}^*)(\eta^6, \eta^1\text{-Bu}^2_2\{\text{CMe}_2\text{CH}_2\}\text{C}_6\text{H}_3)\text{H}]$ has thus been ascribed to direct insertion of a naked scandium atom into a methyl group of free Bz^* in the low temperature matrix. The latter, bond-breaking, process would be expected to be more kinetically favourable at the higher co-condensation temperature from activation energy considerations.

4.3.2 Bonding

The bonding in the $[\text{Ln}(\eta\text{-Bz}^*)_2]$ compounds has been analysed²³ by analogy with that of the parent bis(η -arene) metal compound, $[\text{Cr}(\eta\text{-C}_6\text{H}_6)_2]$, the molecular orbital diagram for the latter is shown in Figure 4.

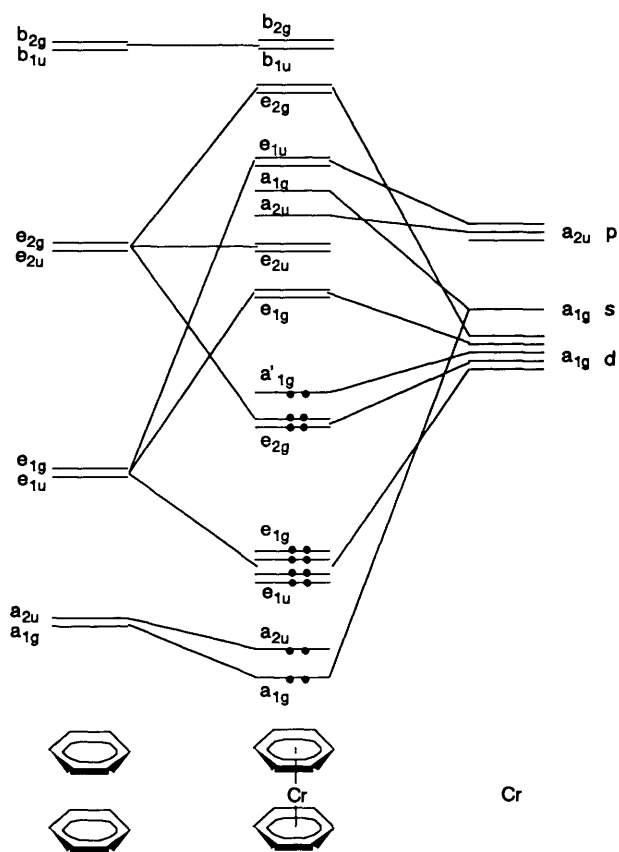


Figure 4 MO Diagram for $[\text{Cr}(\eta\text{-C}_6\text{H}_6)_2]$

The predominantly ring e_{1u} and e_{1g} , and predominantly metal e_{2g} and a_{1g} molecular orbitals are completely filled in an 18-electron compound. Physical studies on the 18-electron bis(η -arene) transition metal sandwich complexes have revealed that the HOMO's are the largely metal-based a_{1g} and e_{2g} orbitals.²⁶ The latter are lower in energy and more delocalized onto the arene rings than the a_{1g} electrons.

The same molecular orbital diagram has been applied to the 15-electron complexes $[\text{Sc}(\eta\text{-Bz}^*)_2]$ and $[\text{Y}(\eta\text{-Bz}^*)_2]$, it can be seen that, by successive filling of the energy levels, there are three electrons in the degenerate e_{2g} levels, and the compounds have 2E ground states. This is in accord with their ESR behaviour

(*vide supra*) and effective magnetic moments (see Section 4.3.3), corresponding to one unpaired electron. Application of the same bonding model to the lanthanide compounds led to the idea that three electrons are required from the lanthanide metal to contribute to the e_{2g} orbitals in order to form a stable compound.

By analogy with $[\text{Sc}(\eta\text{-Bz}^*)_2]$ and $[\text{Y}(\eta\text{-Bz}^*)_2]$, it has been proposed that, to a first approximation, a d^1s^2 configuration is required in either the ground or an easily accessible excited state of the lanthanide atom to form a stable bis(η -arene) complex. Figure 5 shows the promotion energies for the $f^n s^2 \rightarrow f^{n-1} d^1 s^2$ transition in the lanthanides.

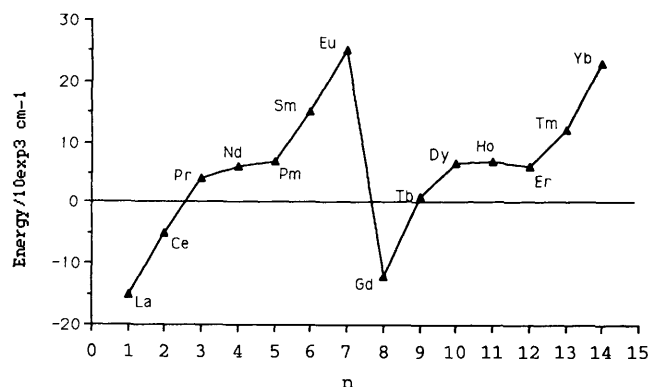


Figure 5 The $f^n s^2 \rightarrow f^{n-1} d^1 s^2$ transition in the lanthanide elements

From the diagram, it appears that Sm, Eu, Tm, and Yb would be the least likely lanthanides to form stable bis(η -arene) complexes because their $f^n s^2 \rightarrow f^{n-1} d^1 s^2$ promotion energies are relatively high, associated with the stabilities of the f^6 , f^7 , f^3 , and f^4 configurations respectively. The results in Table 1 show that, experimentally, this was found to be the case: the compounds of Er, Tm, and Yb were found to be unisolable, and the samarium analogue decomposed to the free metal and ligand above -30°C . In these cases the instability has thus been attributed to an insufficient gain in metal-arene bond energy to offset the necessary promotion energy. Table 1 also shows an area of instability at the beginning of the lanthanide series which is not explicable by the former argument, since the ground state of both La and Ce is $d^1 s^2$ and the promotion energy of Pr is small (see Figure 5). The instability of these complexes has been attributed to the greater covalent radii of the metals, and consequently the Bz^* ligand is not sufficiently bulky to stabilize the metal centre kinetically. (See p. 24 – note added in proof.)

4.3.3 Magnetism

The solid-state magnetic moments have been determined for all the thermally stable $[\text{Ln}(\eta\text{-Bz}^*)_2]$ compounds (see Table 2), and their magnetic properties used as a testing ground for the bonding model discussed in Section 4.3.2.²³ Three magnetic coupling schemes for the interaction between the three e_{2g} electrons and the f electrons have been proposed, on the initial assumption that the orbital angular momentum of the three e_{2g} electrons is quenched, as indicated by the near spin-only moments found for $[\text{Y}(\eta\text{-Bz}^*)_2]$ and $[\text{Sc}(\eta\text{-Bz}^*)_2]$, and the proximity of the g -values to g_e in their ESR spectra.

- (i) The e_2 electrons precess independently with the magnetic field, *i.e.*

$$\text{spin coupling} < kT$$

$$\mu_{\text{eff}} = [3 + g_J^2 J(J+1)]^{1/2}$$

in which the first term in μ arises from the single d electron contribution and g_J is derived by the normal rules for the f^n configuration.

- (ii) That the e_2 electron spin aligns with the spins of the f

electrons, the total spin couples with the orbital angular momentum, and the total angular momentum precesses with the field. This assumes

$$\text{spin coupling} \gg \text{LS coupling}$$

and leads to values of the total spin of $S^* = (S + 1/2)$, orbital angular momentum of $L^* = L$, and total angular momentum of $J^* = (J + 1/2)$ [S, L , and J are the values for the f^n configuration].

$$\mu_{\text{eff}} = g[J^*(J^* + 1)]^{1/2}$$

$$g = 1 + \frac{J^*(J^* + 1) + S^*(S^* + 1) - L^*(L^* + 1)}{2J^*(J^* + 1)}$$

(iii) The e_2 electron spin couples with the total angular momentum of the f electrons, *i.e.*

$$kT < \text{spin coupling} < \text{spin-orbit coupling}$$

$$\mu_{\text{eff}} = g_K[K(K + 1)]^{1/2}$$

$$K = J \pm \frac{1}{2}, \text{ and } g_K = g_J \pm \frac{(g_J - 2)}{(2J + 1)}$$

In fact, calculations have shown that cases (ii) and (iii) give identical predictions for the magnetic moments of all the compounds considered in Table 2.

Table 2 Predicted and experimental magnetic moments for $[\text{Ln}(\eta\text{-Bz}^*)_2]$ compounds

Metal	Atomic Configuration	$\mu_{\text{eff}}/\text{BM}$				Expt.
		Free Atom	Ln^{3+}	Case (i)	Cases (ii) and (iii)	
Sc	d^1s^2		0	1.73	1.73	1.91
Y	d^1s^2		0	1.73	1.73	1.74
Nd	f^4s^2	2.68	3.62	4.01	2.68	1.57 ^a
Gd	$f^7d^1s^2$	6.51	7.94	8.12	8.94	8.75
Tb	f^9s^2	10.64	9.7	9.87	10.74	10.69
Dy	$f^{10}s^2$	10.61	10.64	10.79	11.67	11.20
Ho	$f^{11}s^2$	9.58	10.61	10.75	11.63	10.10
Er	$f^{12}s^2$	7.56	9.58	9.74	10.61	11.00 ^b
Lu	$f^{14}d^1s^2$		0	1.73	1.73	1.69

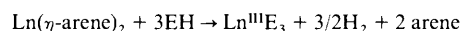
^a The value given is that at < 20 K. At temperatures > 200 K a value of 5.3 was found for μ . ^b The value given is that at < 125 K. At temperatures > 200 K a value of 9.7 was found for μ .

The values predicted by these various coupling schemes are given in Table 2, together with the values for the free atoms (where known), those for the Ln^{3+} ions, and the experimental values for the compounds. Overall the divergence of the experimental results from the free atom values is large, indicating significant perturbation of the atomic f -shell on bonding of the arene rings to the lanthanide atom. The experimental values tend to lie between the two values predicted by cases (ii) and (iii), and case (i), except for Ho where the experimental moment is less than expected on either basis. For Er two values of μ were found, depending on the temperature: in the low temperature region (< 125 K) μ lies near the value for the two coupled schemes, but at temperatures > 200 K is very close to the uncoupled scheme where kT is assumed to be significantly greater than the spin coupling. A similar situation occurs for Nd, although the discrepancy between the experimental and predicted values of μ is somewhat greater.

Overall, the above results have been taken as a corroboration of the promotion energy model discussed earlier.

4.3.4 Reaction Chemistry

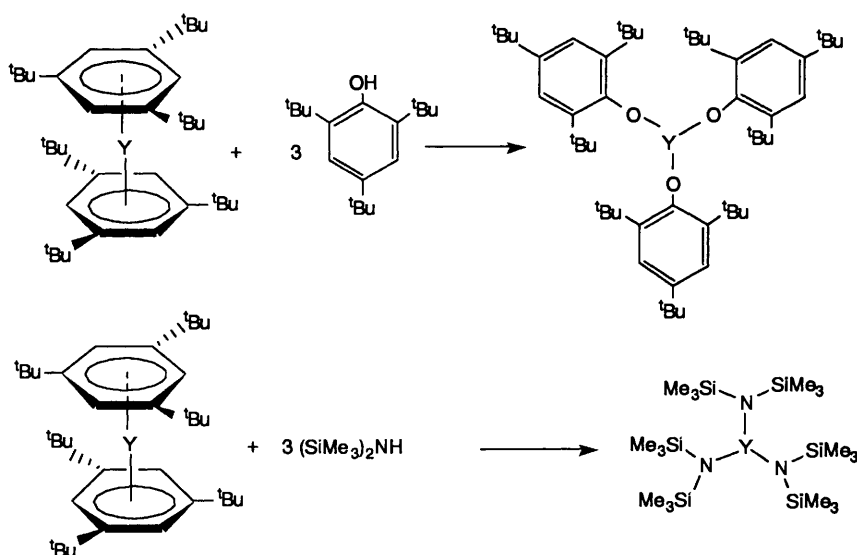
4.3.4.1 Redox reactions. As might be anticipated with metal (0) complexes of very electropositive elements, the $[\text{Ln}(\eta\text{-Bz}^*)_2]$ compounds have been found to undergo facile reaction with substrates possessing acidic hydrogens to generate lanthanide(III) species, *i.e.*



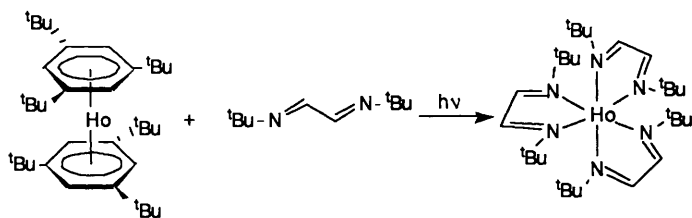
Thus reaction of $[\text{Y}(\eta\text{-Bz}^*)_2]$ with 2,4,6-tri-*t*-butylphenol or hexamethyldisilazane afforded the tris(aryloxyde)²⁷ and tris(bis(trimethylsilyl)amide)²⁸ Y^{III} derivatives respectively²⁹ (Scheme 5).

4.3.4.2 Ring displacement reactions. Bis(η -arene) transition metal complexes, *e.g.* Mo and W, have been shown to undergo a variety of ring displacement reactions with neutral two-electron donors such as phosphines or carbon monoxide.⁵ Analogous reactions with the $[\text{Ln}(\eta\text{-Bz}^*)_2]$ compounds resulted in decomposition and concomitant decomposition of the free metal, possibly *via* initial formation of an unstable adduct, although no spectroscopic evidence could be found for such a species, *e.g.* low temperature IR studies in the case of reactions with CO.¹⁸

However, a photochemically driven reaction between $[\text{Ho}(\eta\text{-Bz}^*)_2]$ and Bu¹DAB has been found to yield $[\text{Ho}(\text{Bu}^1\text{DAB})_3]$



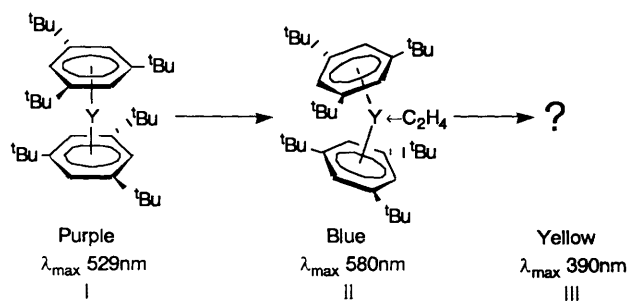
Scheme 5



Scheme 6

(Scheme 6), the latter is also accessible directly from holmium atoms and Bu^tDAB (see Section 4.2), and its formation from [Ho(η-Bz*)₂] has been attributed to the superior π-acceptor abilities of Bu^tDAB versus Bz*.

4.3.4.3 Ethene polymerization The [Ln(η-Bz*)₂] compounds have been found to be very active, homogeneous catalysts for ethene polymerization in hydrocarbon solvents.³⁰ They produce very high density, narrow molecular weight distribution polyethene, with turnover numbers in excess of 10⁴. The activity of these systems was found to be dependent on the particular lanthanide, those at the beginning of the lanthanide series giving higher polymerization rates, associated with their greater size. IR and solid-state NMR studies showed there to be minimal branching in the polyethene and this was taken to be indicative of a genuine homogeneous process and to mitigate against a free radical mechanism. Low temperature studies on the yttrium system (see Scheme 7) showed that, after initial ethene uptake, a blue species (II) was produced which then underwent rapid reaction to give a yellow species (III), the active catalyst. The ESR spectrum of the blue species indicated a slightly distorted [Y(η-Bz*)₂] fragment, which has been tentatively ascribed to a simple ethene adduct. The nature of the subsequent yellow product remains unknown, although a vinyl hydride would be a reasonable candidate.



Scheme 7

4.4 Reactions of Scandium, Yttrium, and Lanthanide Atoms with other Arenes

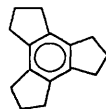
The reactions of yttrium atoms with arenes less sterically demanding than tri-*t*-butylbenzene (toluene, mesitylene, and 1,3,5-triisopropylbenzene) have been examined.¹⁸ In the case of both toluene and mesitylene, the intense purple matrix formed during the co-condensation experiment did not survive above ca. 120 K, whilst bis(η-1,3,5-triisopropylbenzene)yttrium was found to be thermally unstable above 270 K, and could only be characterized in solution by ESR and visible spectroscopy. The stability of the tri-*t*-butylbenzene derivatives has thus been attributed to the steric saturation achieved by the ligand, but also to the increase in metal–arene bond strength arising from the positive inductive effect of the *t*-butyl ring substituents.

The effect of the ring substituents on the stability, charge-transfer band and electronic ground state of bis(η-arene)scandium(0) complexes has been studied in some detail, and the results are shown in Table 3.²⁰

Overall, there is a good correlation between the bulk of the arene and the thermal stability of the resultant bis(η-arene)scandium(0) complex, and the smaller size of scandium compared with yttrium and the lanthanides results in relatively more stable products even with quite small arenes (e.g. mesitylene). There is also a trend for a shift of λ_{max} to longer wavelength (i.e. lower energy) with increasing alkyl substitution (and hence +I effect) of the rings. Thus, this charge-transfer band has been assigned as ligand-to-metal in character, and, *inter alia*, also that in the yttrium and lanthanide analogues. Given the electron-rich nature of the metal centres in these compounds, this assignment seems counter-intuitive at first sight, but the ²E ground state of these compounds leaves the *d* (a_{1g}) orbital empty, and the latter, which is directed towards the centroids of the two rings in a parallel ring sandwich compound, thus provides a suitable acceptor site for the LMCT transition. However, the trend in λ_{max} is not followed by [Sc(η-1,3,5-Me₃C₆H₃)₂] and [Sc(η-C₆Me₅H)₂], and, moreover, the latter were both found to be ESR-silent, even at 4 K. These observations have been rationalized in terms of the adoption of the high-spin ⁴A/(e_{2g}² a_{1g}¹) ground state by [Sc(η-1,3,5-Me₃C₆H₃)₂] and [Sc(η-C₆Me₅H)], as opposed to the ²E state (e_{2g}³) adopted by the remaining bis(η-arene) scandium(0) complexes. The ⁴A ground state is adopted by the isoelectronic vanadocene complexes,³¹ and ground state changes as a result of ring alkylation have been previously observed in manganocene derivatives.³²

Table 3 Selected data for bis(η-arene) scandium(0) complexes

Arene	Stability	λ _{max} (nm) ^a	ESR behaviour ^b
1,3,5-Me ₃ C ₆ H ₃	dec > -30 °C	523	silent
C ₆ Me ₅ H	dec > 0 °C	534	silent
1,4-Bu ^t ₂ C ₆ H ₄	dec > 100 °C	467	active
C ₆ Me ₆ ^c	dec > 40 °C	494	active
1,3,5-Bu ^t ₃ C ₆ H ₃	dec > 120 °C	495	active

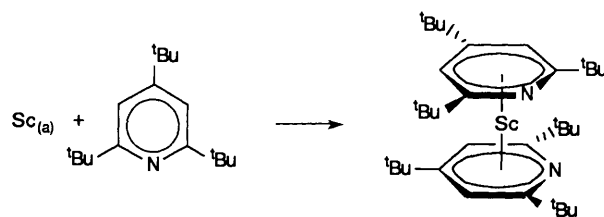


(trindan)

1,3,5-Bu ^t ₃ -4-MeC ₆ H ₂	dec > 100 °C	500	active
2,4,6-Bu ^t ₃ C ₅ H ₂ N	dec > 120 °C	503	active
	dec > 100 °C	470	active

^a Pentane solution ε > 10⁴ ^b Frozen solution at 77 K ^c Characterized in solution only

Table 3 also includes data for [Sc(η-2,4,6-Bu^t₃C₅H₂N)₂], the first heteroatom-substituted Sc⁰ sandwich complex, prepared by co-condensation of scandium vapour with 2,4,6-tri-*t*-butylpyridine (Scheme 8).²⁰



Scheme 8

5 Conclusions

The existence of stable, unambiguous zero oxidation state complexes of scandium, yttrium, and the lanthanide elements is now well-established with the synthesis of bis(η-arene) compounds of these very electropositive metals. Their reaction chemistry is clearly rather different from that of the *d*-block analogues, and offers considerable scope for further study. There also remains the challenge of finding other ligand environments to stabilize lanthanide(0) compounds, and of extending zero oxidation state chemistry of the *f*-elements to the actinides, thorium and uranium.

6 References

- 1 H Schumann, *Angew Chem Int Edn Engl*, 1984, **23**, 474
- 2 H B Kagan, *Nouv J Chem*, 1990, **14**, 453
- 3 W J Evans, *Polyhedron*, 1987, **6**, 803, and references therein
- 4 A Greco, S Cesca, and G Bertoloni, *J Organomet Chem*, 1976, **113**, 321
- 5 W E Silverthorn, *Adv Organomet Chem*, 1975, **13**, 47
- 6 F A Cotton and W Schwotzer, *J Am Chem Soc*, 1986, **108**, 4657
- 7 G B Deacon, A J Kopllick, and T D Tuong, *Polyhedron*, 1982, **1**, 423
- 8 G B Deacon, P I Mackinnon, and T D Tuong, *Aust J Chem*, 1983, **36**, 43
- 9 R K Shelton and J L Slater, *Angew Chem Int Edn Engl*, 1975, **14**, 309
- 10 M P Andrews and A L Wayda, *Organometallics*, 1988, **7**, 743
- 11 J A Howard, B Mile, C A Hampson, and H Morris, *J Chem Soc Faraday Trans*, 1989, **85**, 3953
- 12 F G N Cloke and M L H Green, *J Chem Soc Dalton Trans*, 1981, 1938
- 13 F G N Cloke, K Courtney, A A Sameh, and A C Swain, *Polyhedron*, 1989, **8**, 1641
- 14 P L Timms and T W Turney, *Adv Organomet Chem*, 1977, **15**, 33, M L H Green, *J Organomet Chem*, 1980, **200**, 119, F G N Cloke, submitted to *Chem Rev*
- 15 G van Koten and K Vrieze, *Adv Organomet Chem*, 1982, **21**, 151
- 16 F G N Cloke, H C de Lemos, and A A Sameh, *J Chem Soc Chem Commun*, 1986, 1344
- 17 F G N Cloke and A A Sameh, unpublished results
- 18 A A Sameh, D Phil Thesis, University of Sussex, 1990
- 19 R A Andersen, F G N Cloke, and C I Dalby, unpublished results
- 20 K Khan, D Phil, Thesis, University of Sussex 1991
- 21 F G N Cloke, C I Dalby, M J Henderson P B Hitchcock C H L Kennard, R N Lamb, and C L Raston, *J Chem Soc Chem Commun*, 1990, 1394, F G N Cloke, C I Dalby, P J Daff and J C Green, *J Chem Soc Dalton Trans*, 1991, 181
- 22 J Brennan, F G N Cloke, A A Sameh and A Zalkin *J Chem Soc Chem Commun* 1987 1669
- 23 D M Anderson, F G N Cloke, P A Cox, N Edelstein J C Green, T Pang, A A Sameh, and G Shalimoff, *J Chem Soc Chem Commun* 1989 53
- 24 E Kevlin and F Jellinek, *J Organomet Chem* 1966, **5**, 490, E Forster, G Albrecht, W Dursten, and E Kurras, *ibid*, 1969, **19**, 215 A Haarland, *Acta Chem Scand*, 1965 **19**, 41
- 25 F G N Cloke, K Khan and R N Perutz, *J Chem Soc Chem Commun*, 1991, 1372
- 26 F G N Cloke, A N Dix, J C Green R N Perutz and E A Seddon, *Organometallics*, 1983, **2**, 1150
- 27 P B Hitchcock, M F Lappert, and R G Smith, *Inorg Chem Acta* 1987, **139**, 183
- 28 D C Bradley, J S Ghotra, and F A Hart *J Chem Soc Dalton Trans*, 1973, 1021
- 29 D M Anderson and F G N Cloke unpublished results
- 30 D M Anderson, F G N Cloke, and D J Duncalf, unpublished results
- 31 J C Green, *Struct Bonding*, 1981, **43**, 37
- 32 J L Robbins, N M Edelstein, S R Cooper, and J C Smart, *J Am Chem Soc*, 1979, **101**, 3853 J H Ammeter, R Bucher and N Oswald, *J Am Chem Soc*, 1974, **96**, 7833

Note added in proof the thermochemical lanthanide arene bond energies for several of the $[\text{Ln}(\eta\text{-Bz}^*)_2]$ complexes have recently been reported and the results are in good agreement with the promotion energy model, W A King, T J Marks, F G N Cloke, and D J Duncalf, *J Am Chem Soc*, 1992, **114**, 9221